Inorg. Chem. **2005**, *44*, 9154–9161

Crystal Structures and Magnetic Properties of Mixed Iridium–Ruthenium Triple Perovskites. 2. $Ba_3MRuIrO_9$ (M = Li, Na, Mg, Ni, Zn, Bi, In)

Michael W. Lufaso and Hans-Conrad zur Loye*

Department of Chemistry and Biochemistry, University of South Carolina, Columbia, South Carolina 29208

Received August 5, 2005

Crystal structures and magnetic properties of polycrystalline $Ba_3MRuIrO_9$ (M^{1+} = Li, Na; M^{2+} = Mg, Ni, Zn; M^{3+} = Bi, In) were investigated. Rietveld refinements of the crystal structures using powder diffraction data indicate that, with the exception of $Ba_3BiRuIrO_9$, all compounds crystallize in the 6H-$BaTiO_3$ structure type in space group $P6_3/mmc$; $Ba_3BiRuIrO_9$ crystallizes in space group $C2/c$. The 6H-$BaTiO_3$, or triple-perovskite, structure is composed of hexagonal and cubic stacking of $[AO_3]$ layers and contains face- and corner-sharing octahedra. The structures in this study contain a disordered mixture of Ir and Ru in the face-sharing octahedra dimers, which are connected via corner-shared MO_6 octahedra. Magnetic susceptibility measurements as a function of temperature were carried out on each compound. Effective magnetic moments were smaller than values estimated using spin-only moments, which indicate the presence of spin–orbit coupling and strong interactions in the face-sharing octahedra that contain a disordered mixture of Ru and Ir on a single crystallographic site. Over a broad temperature range, a divergence of the zero-field-cooled and field-cooled data were observed for $Ba_3MgRuIrO_9$, $Ba_3NiRuIrO_9$, $Ba_3ZnRuIrO_9$, and $Ba_3LiRuIrO_9$.

1. Introduction

In part 1 of this article, perovskites and perovskite-related oxides containing Ir or Ru were noted to exhibit interesting structural variations and diverse physical properties. Investigations of these properties rely on a solid understanding of the structural variations that exist within this family of compounds.[1,2] One specific class of quaternary oxides $Ba_3MRu_2O_9$ and $Ba_3MIr_2O_9$ (M = alkali, alkaline earth, transition metal, and lanthanide cations), known as triple perovskites, have been the subject of numerous investigations concerning their structures and magnetic properties.[3−12] Several compounds adopt closely related crystal structures that have the same polyhedral connectivity as the 6H-$BaTiO_3$-type structure; however, they crystallize in different space groups and include $Ba_3BiIr_2O_9$, $Ba_3LaIr_2O_9$, and $Ba_3NdIr_2O_9$, which crystallize in space group $C2/c$.[7] Some compounds undergo structural transitions and change space groups upon heating or cooling. For example, $Ba_3NaRu_2O_9$ undergoes charge ordering of the Ru^{5+} and Ru^{6+} transition at 210 K and a concomitant phase transition from $P6_3/mmc$ to space group $Cmcm$.[13] Additionally, $Ba_3CuRu_2O_9$ crystallizes in space group $Cmcm$ at ambient temperatures,[14] whereas $Ba_3CoRu_2O_9$ undergoes a phase transition from $P6_3/mmc$ at room temperature to space group $Cmcm$ at 2 K.[15]

Magnetic properties in the all-ruthenium or all-iridium series of triple perovskites $Ba_3MRu_2O_9$ and $Ba_3MIr_2O_9$ are

* Author to whom correspondence should be addressed. Tel.: (803) 777-6916. Fax: (803) 777-8508. E-mail: zurloye@mail.chem.sc.edu.

(1) Mitchell, R. H. *Perovskites: Modern and Ancient*; Almaz Press: Ontario, Canada, 2002.
(2) Cava, R. J. *Dalton Trans.* **2004**, 2979.
(3) Doi, Y.; Wakeshima, M.; Hinatsu, Y.; Tobo, A.; Ohoyama, K.; Yamaguchi, Y. *J. Mater. Chem.* **2001**, *11*, 3135.
(4) Doi, Y.; Hinatsu, Y.; Shimojo, Y.; Ishii, Y. *J. Solid State Chem.* **2001**, *161*, 113.
(5) Doi, Y.; Hinatsu, Y. *J. Solid State Chem.* **2004**, *177*, 3239.
(6) Hinatsu, Y.; Oyama, S.; Doi, Y. *Bull. Chem. Soc. Jpn.* **2004**, *77*, 1479.
(7) Doi, Y.; Hinatsu, Y. *J. Phys.: Condens. Matter* **2004**, *16*, 2849.
(8) Doi, Y.; Matsuhira, K.; Hinatsu, Y. *J. Solid State Chem.* **2002**, *165*, 317.
(9) Doi, Y.; Wakeshima, M.; Hinatsu, Y.; Tobo, A.; Ohoyama, K.; Yamaguchi, Y. *J. Alloys Compd.* **2002**, *344*, 166.
(10) Gonen, Z. S.; Gopalakrishnan, J.; Eichhorn, B. W.; Greene, R. L. *Inorg. Chem.* **2001**, *40*, 4996.
(11) Darriet, J.; Bontchev, R.; Dussarrat, C.; Weill, F.; Darriet, B. *Eur. J. Solid State Inorg. Chem.* **1993**, *30*, 273.
(12) Thumm, I.; Treiber, U.; Kemmler-Sack, S. *J. Solid State Chem.* **1980**, *35*, 156.
(13) Stitzer, K. E.; Smith, M. D.; Gemmill, W. R.; zur Loye, H. C. *J. Am. Chem. Soc.* **2002**, *124*, 13877.
(14) Rijssenbeek, J. T.; Huang, Q.; Erwin, R. W.; Zandbergen, H. W.; Cava, R. J. *J. Solid State Chem.* **1999**, *146*, 65.
(15) Lightfoot, P.; Battle, P. D. *J. Solid State Chem.* **1990**, *89*, 174.

10.1021/ic051345r CCC: $30.25
Published on Web 11/12/2005

the result of the interactions between the Ru ions in the $[Ru_2O_9]$ dimer or the Ir ions in the $[Ir_2O_9]$ dimer and the interaction between the M and Ru or M and Ir ions along the linear M−O−Ru or M−O−Ir pathway.[16] In the 6H-$BaTiO_3$ and related structures, the short Ru−Ru and Ir−Ir bond distances (2.5−2.8 Å) in the face-sharing dimer promote strong orbital interactions between the magnetic cations. In this paper, we report the crystal chemistry and magnetic properties measured between 2 and 300 K for a mixed ruthenium−iridium triple-perovskite series, $Ba_3MRuIrO_9$ (M = Li, Na, Mg, Ni, Zn, Bi, In).

2. Experimental Section

Black polycrystalline samples were prepared by conventional solid-state methods. RuO_2 was prepared from Ru metal (Engelhard, 99.5%) by heating it in air to 950 °C for 48 h with an intermediate grinding. The starting reactant materials were $BaCO_3$ (Alfa Aesar, 99.95%), Ir (Engelhard, 99.5%), Na_2CO_3 (Alfa Aesar, 99.997%), Li_2CO_3 (Johnson Matthey, 99.999%), MgO (Alfa Aesar, 99.998%), NiO (Alfa Aesar, 99.998%), ZnO (Aldrich, 99.9%), In_2O_3 (Alfa Aesar, 99.999%), and Bi_2O_3 (Alfa Aesar, 99.975%). The starting materials were weighed in the correct ratios and ground in an agate mortar with acetone. The samples were calcined overnight in high-form alumina crucibles. Successive heating, to the temperature given in parentheses, and grinding cycles were performed in flowing O_2 for $Ba_3LiRuIrO_9$ (850 °C) and $Ba_3NaRuIrO_9$ (850 °C) and in air for $Ba_3MgRuIrO_9$ (1100 °C), $Ba_3NiRuIrO_9$ (1050 °C), $Ba_3ZnRuIrO_9$ (850 °C), $Ba_3BiRuIrO_9$ (950 °C), and $Ba_3InRuIrO_9$ (1000 °C). Heating cycles of the samples were continued for between 2 and 10 days until changes in the weakest peaks were no longer evident and equilibrium was achieved.

X-ray powder diffraction data were collected using a Rigaku DMAX 2200 diffractometer. Data were collected at 0.03° steps for 12.5 s/step over the 2θ range 5−110°. Rietveld refinements were performed using the EXPGUI GSAS package.[17,18] Magnetic susceptibility measurements were made using a Quantum Design MPMS XL SQUID magnetometer. The powder samples were placed inside a gelatin capsule and inserted into a plastic straw. The small diamagnetic contribution of the gelatin capsule had a negligible contribution to the overall magnetization, which was dominated by the sample. Data were collected after cooling in the absence of an applied field [zero-field cooled (ZFC)] and after cooling in a magnetic field [field cooled (FC)] of 1 kG.

3. Results and Discussion

3.a. Crystal Structures. Systematic absences in the intensity data were consistent with the space group $P6_3/mmc$ for each compound except for $Ba_3BiRuIrO_9$. Similar to $Ba_3BiRu_2O_9$, which crystallizes[11] in space group $C2/c$, $Ba_3BiRuIrO_9$ could be indexed in the monoclinic space group $C2/c$ with $a_m \sim a_h$, $b_m \sim \sqrt{3}b_h$, $c_m \sim c_h$, and $\beta \sim 90°$, where subscripts m and h refer to the monoclinic and hexagonal unit cells, respectively. The large ionic radius, 1.03 Å, of Bi^{3+} in a six-coordinate environment is comparable to, but slightly smaller than, the 1.032 Å reported for La^{3+}.[19] In the accompanying article (part 1 of this study), $Ba_3LaRuIrO_9$ was found to crystallize in space group $P6_3/mmc$. Size differences alone cannot account for the difference observed in the crystal structures but may be driven by the presence of a stereochemically active lone pair of the bismuth cation. Three distinct Bi−O bond distances are present in the structure crystallizing in space group $C2/c$, in contrast to the six equidistant bonds in the octahedral coordination in the $P6_3/mmc$ structure. For the nonspherically symmetric Bi^{3+} cation, occupation of a slightly distorted octahedral coordination environment in space group $C2/c$ appears to be favored over the symmetric environment in $P6_3/mmc$.

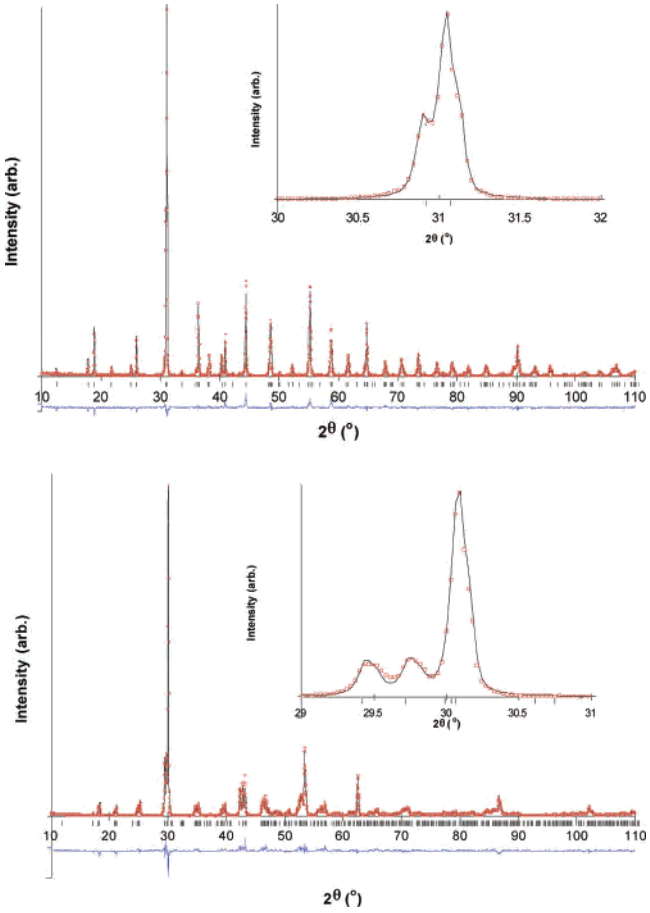

Figure 1. Ambient temperature X-ray powder diffraction data for $Ba_3NiRuIrO_9$ (top) and $Ba_3BiRuIrO_9$ (bottom). Circles are collected data; solid lines are fitted. Differences between observed and calculated intensities are shown below. Vertical marks indicate allowed peak positions.

A majority of $Ba_3MIr_2O_9$ and $Ba_3MRu_2O_9$ compounds crystallize in space group $P6_3/mmc$,[7,8,13,20] and hence, it is not surprising that the mixed Ru/Ir analogues crystallize in the same space group. X-ray diffraction profiles for $Ba_3NiRuIrO_9$ and $Ba_3BiRuIrO_9$ are shown in Figure 1. The insets show the splitting of the strongest reflections, which are indicative of monoclinic symmetry for $Ba_3BiRuIrO_9$. Crystal structures of hexagonal $Ba_3NiRuIrO_9$ and monoclinic $Ba_3BiRuIrO_9$ are shown in Figure 2. In $Ba_3NiRuIrO_9$, the corner-sharing octahedral site is occupied by Ni and the face-sharing octahedral site is occupied by a disordered mixture

(16) Darriet, J.; Dillon, M.; Villeneuve, G.; Hagenmuller, P. *J. Solid State Chem.* **1976**, *19*, 213.
(17) Larson, A. C.; von Dreele, R. B. *General Structure Analysis System (GSAS)*; Los Alamos National Laboratories: Los Alamos, NM, 1990.
(18) Toby, B. H. *J. Appl. Crystallogr.* **2001**, *34*, 210.
(19) Shannon, R. D. *Acta Crystallogr., Sect. A* **1976**, *32*, 751.
(20) Kim, S. J.; Smith, M. D.; Darriet, J.; zur Loye, H. C. *J. Solid State Chem.* **2004**, *177*, 1493.

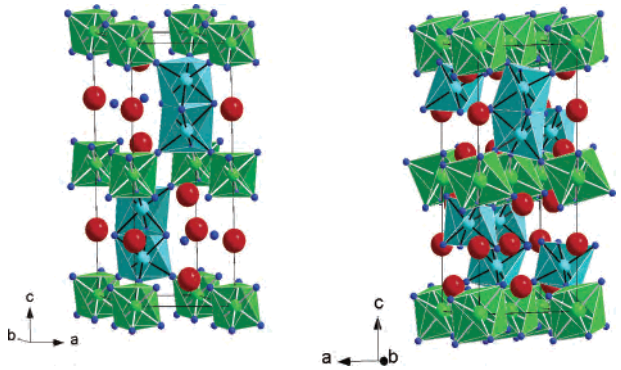

Figure 2. Crystal structures of $Ba_3NiRuIrO_9$ (left) and $Ba_3BiRuIrO_9$ (right) consisting of $(Ru/Ir)O_6$ (cyan) face-sharing bioctahedra corner-shared to LaO_6 or BiO_6 (green) octahedra. Barium cations are shown as red spheres and oxygen atoms as blue spheres.

Table 1. Fractional Atomic Coordinates and Isotropic Thermal Parameters for $Ba_3BiRuIrO_9$[a]

	x	*y*	*z*	Ui/Ue*100
Ba1	0	−0.0035(8)	1/4	0.44(16)
Ba2	0.0093(7)	0.3328(7)	0.0961(2)	0.87(13)
Bi1	0	0	0	0.31(7)
Ru/Ir	−0.0119(6)	0.3347(7)	0.8367(2)	0.31(7)
O1	0	0.489(6)	1/4	0.31(7)
O2	0.275(6)	0.760(4)	0.261(2)	0.31(7)
O3	0.826(6)	0.593(4)	0.062(2)	0.31(7)
O4	0.048(7)	0.826(5)	0.092(2)	0.31(7)
O5	0.293(7)	0.605(4)	0.110(2)	0.31(7)

[a] Space group *C*2/*c*, $a = 5.9480(5)$ Å, $b = 10.2847(9)$ Å, $c = 14.8080(14)$ Å, $\beta = 91.313(3)°$. Selected bond lengths: Bi−O3, 2.33(4) Å; Bi−O4, 2.26(4) Å; Bi−O5, 2.32(4) Å; (Ru/Ir)−O1, 2.22(5) Å; (Ru/Ir)−O2, 2.32(3) Å; (Ru/Ir)−O2, 2.29(4) Å; (Ru/Ir)−O3, 1.99(4) Å; (Ru/Ir)−O4, 1.98(4) Å; (Ru/Ir)−O5, 1.97(4) Å. $R_{wp} = 16.63\%$, $R_p = 12.71\%$, $R(F^2) = 9.66\%$, $\chi^2 = 3.31$.

of Ru and Ir. $Ba_3BiRuIrO_9$ has the same atom connectivity and is structurally related to the phase that crystallizes in space group $P6_3/mmc$. Similarly, bismuth is located in the corner-sharing octahedral site, while the face-sharing octahedral site is occupied by a disordered mixture of Ru and Ir. In each crystal structure, the barium atoms are located in 12-fold coordination sites. Refinements in space group $P6_3/mc$, which allows for an ordered arrangement of Ru and Ir in the face sharing dimer, did not result in an improvement of the fit. This is not unexpected, as only a slight difference exists between the ionic radii of Ru^{4+} (0.62 Å) and Ir^{4+} (0.625 Å) and between those of Ru^{5+} (0.565 Å) and Ir^{5+} (0.57 Å).[19] The absence of long-range order in the cation arrangement of Ru and Ir in the face-sharing octahedra was indicated in the structure refinements of these compounds.

Refined fractional coordinates of the Rietveld refinements for $Ba_3BiRuIrO_9$ are given in Table 1 and those for the remaining compounds in Table 2. Selected bond distances are given in Table 3. A careful view should be taken in analyzing the O positions and bond distances in these refinements as an accurate determination of the (Ru/Ir)−O and M^{n+}−O bond lengths from X-ray powder diffraction measurements is difficult. The disordered mixture of Ru and Ir on a single crystallographic site and the inherent difficulty in accurately locating the weakly scattering O nearby electron-dense cations, such as Ba and Ir, lead to the likelihood of a larger uncertainty in the position than indicated by the refinements. Some minor differences were evident in the trends of the difference between the long and short (Ru/Ir)−O bond distances in $Ba_3LiRuIrO_9$ [1.940(11) and 2.019(11) Å], which were less than Ir−O bond lengths in $Ba_3LiIr_2O_9$ [1.878(6) and 2.040(4) Å][20] and $Ba_3LiRu_2O_9$ [1.852(3) and 2.039(3) Å][13] that were both determined from single-crystal X-ray diffraction analyses. The average bond lengths, however, are comparable with $d(Ir-O) = 1.95$ Å in $Ba_3LiRu_2O_9$ and $d(Ru-O) = 1.96$ Å in $Ba_3LiRu_2O_9$ versus an average (Ru/Ir)−O length of 1.98 Å in $Ba_3LiRuIrO_9$. The trend of a reduced difference between the short and long (Ru/Ir)−O bond lengths is noticeable throughout the entire series of $Ba_3MRuIrO_9$ compounds; however, to verify the subtle differences in the bond lengths between the mixed iridate−ruthenates in this study and the end member ruthenate or iridate triple perovskites examined previously, single-crystal X-ray or neutron powder diffraction data would be needed.

The presence of short and long bond distances in the face-sharing site is typical for triple perovskites. The long (Ru/Ir)−O distance is to the oxygen that is in the shared face, and the short (Ru/Ir)−O bond is the one that corner-shares to the M cation. A distortion of the octahedra by the formation of three long and three short bonds may be predicted by considering the connectivity of the atoms in the crystal structure. Using Pauling's rules[21] and assuming equidistant bonds in the first coordination sphere of the octahedra, each cation−anion bond contributes a quantity (valence units, v.u.) equal to the oxidation state divided by the coordination number to the total cation bond valence sums (BVS).[21] For example, consider a general compound $Ba_3M^{2+}RuIrO_9$, where the average oxidation state of (Ru/Ir) is pentavalent. In an undistorted octahedra, the $(Ru/Ir)O_6$ has six equidistant (Ru/Ir)−O bonds, each with a valence of 5/6 v.u. The $M^{2+}O_6$ has six equidistant M^{2+}−O bonds, each contributing 2/6 v.u. Each O is bonded to four 12-coordinated barium atoms, each contributing 2/12 to the valence sum. The sum of the six bonds of the octahedral cations gives a BVS equal to the formal oxidation state using the assumption of undistorted octahedra. However, in the triple perovskites, there is an asymmetry in the bond network for the two distinctly coordinated oxygen anions, the first, O1, bonded to two (Ru/Ir) and the second, O2, bonded to one (Ru/Ir) and one M^{2+}. The valence sum of O1 is $5/6 + 5/6 + 4 \times 2/12 = 2\,1/3$ v.u., which is slightly overbonded compared to the ideal valence of 2 v.u. for oxygen. The valence sum of O2 is $5/6 + 2/6 + 4 \times 2/12 = 1\,5/6$, which is slightly underbonded. To obtain an ideal coordination for the oxygen atoms, the (Ru/Ir)−O1 distances may lengthen and the (Ru/Ir)−O2 distances may shorten to form bonds with valences of 2/3 and 1 v.u., respectively, which results in the valence sums of O1 and O2 becoming equal to 2.0 v.u. and, thus, equivalent to the formal oxidation state. It is this distortion of three long and three short bonds that occurs to relieve the bond strain present for the oxygen in the face-

(21) Pauling, L. *J. Am. Chem. Soc.* **1929**, *51*, 1010.

Table 2. Isotropic Thermal Parameters and Refinement Details and Background Subtracted R_{wp} and R_p Values for the Remaining Compounds[a]

	$Ba_3InRuIrO_9$	$Ba_3NiRuIrO_9$	$Ba_3MgRuIrO_9$	$Ba_3ZnRuIrO_9$	$Ba_3LiRuIrO_9$	$Ba_3NaRuIrO_9$
a (Å)	5.8213(4)	5.753 04(23)	5.7644(3)	5.7784(5)	5.7754(8)	5.868 76(12)
c (Å)	14.3648(12)	14.1901(6)	14.2170(9)	14.2724(14)	14.281(2)	14.5164(3)
vol (Å^3)	421.57(5)	406.73(3)	409.12(4)	412.70(6)	412.54(10)	432.995(16)
Ba2 *z*	0.9105(2)	0.910 99(13)	0.910 78(14)	0.911 09(16)	0.913 43(18)	0.910 79(13)
Ru/Ir *z*	0.160 06(19)	0.153 88(10)	0.154 45(11)	0.154 58(12)	0.152 78(14)	0.155 94(11)
O1 *x*	0.526(2)	0.5059(12)	0.5035(13)	0.5099(13)	0.4798(15)	0.5004(12)
O2 *x*	0.1564(19)	0.1545(9)	0.1455(9)	0.1520(11)	0.1715(11)	0.1593(10)
O2 *z*	0.4127(11)	0.4210(6)	0.4244(6)	0.4192(7)	0.4221(8)	0.4125(6)
Ui/Ue*100 Ba1	−0.13(18)	0.38(8)	1.14(10)	1.03(12)	1.12(10)	0.41(8)
Ui/Ue*100 Ba2	0.53(10)	0.51(5)	0.98(6)	1.11(7)	1.98(7)	0.85(6)
Ui/Ue*100 M	0.5(2)	−0.92(17)	−4.4(2)	0.31(21)	5.1(34)	0.5(4)
Ui/Ue*100 Ru/Ir	−0.25(8)	0.40(5)	0.62(6)	0.57(6)	1.61(7)	0.34(5)
Ui/Ue*100 O1	3.3(11)	−0.6(4)	−0.1(4)	0.8(5)	1.6(5)	−0.6(4)
Ui/Ue*100 O2	−1.8(5)	−0.4(4)	−0.2(3)	0.4(3)	3.0(4)	−0.6(3)
R_{wp} (%)	16.00	12.23	13.10	12.82	14.91	14.35
R_w (%)	12.45	9.47	10.25	10.29	11.49	11.14
$R(F^2)$	9.01	7.06	6.87	6.56	6.22	12.05
χ^2	3.46	2.35	2.65	2.62	3.08	2.56

[a] Atomic coordinates are Ba1(0, 0, $^1/_4$), Ba2($^1/_3$, $^2/_3$, *z*), M(0, 0, 0), Ru/Ir($^1/_3$, $^2/_3$, *z*), O1(*x*, 2*x*, $^1/_4$), and O2(*x*, 2*x*, *z*) in space group $P6_3/mmc$.

Table 3. Selected Interatomic Distances (Å), Angles, and Off-Center Displacements (Δ)

	$Ba_3InRuIrO_9$	$Ba_3MgRuIrO_9$	$Ba_3NiRuIrO_9$	$Ba_3ZnRuIrO_9$	$Ba_3LiRuIrO_9$	$Ba_3NaRuIrO_9$
Ba1−O1 (× 3)	2.922(2)	2.8824(2)	2.8768(3)	2.8906(5)	2.8948(12)	2.934 07(6)
Ba1−O1 (× 3)	2.922(2)	2.8824(2)	2.8774(3)	2.8912(5)	2.8947(12)	2.934 69(6)
Ba1−O2 (× 6)	2.819(16)	2.874(9)	2.874(8)	2.854(10)	2.997(11)	2.860(9)
Ba2−O1 (× 3)	2.709(13)	2.807(8)	2.791(7)	2.784(8)	2.990(10)	2.882(8)
Ba2−O2 (× 3)	2.9124(7)	2.8962(9)	2.8823(6)	2.8949(7)	2.8908(7)	2.9352(3)
Ba2−O2 (× 3)	2.9130(7)	2.8968(9)	2.8829(6)	2.8955(7)	2.8907(7)	2.9358(3)
Ba2−O2 (× 3)	3.105(17)	3.001(9)	2.976(9)	3.027(10)	2.853(11)	3.117(9)
M−O2 (× 6)	2.015(18)	1.807(9)	1.904(9)	1.909(10)	2.045(11)	2.058(9)
Ru/Ir−O1 (× 3)	2.330(19)	2.175(10)	2.194(9)	2.231(11)	2.019(11)	2.178(10)
Ru/Ir−O2 (× 3)	2.068(18)	2.185(9)	2.075(9)	2.098(11)	1.940(11)	2.029(9)
(Ru/Ir)−(Ru/Ir)	2.588(5)	2.717(3)	2.728(3)	2.724(4)	2.777(3)	2.731(3)
(Ru/Ir)−O1−(Ru/Ir)	67.4(5)	77.3(3)	76.9(3)	75.3(3)	86.9(5)	77.6(3)
Δ (Å)	0.095(3)	0.174(2)	0.181(1)	0.173(2)	0.198(2)	0.156(2)

sharing position that is bonded to two higher valence ions and for the outer oxygen which shares a bond to a lower valence ion. The octahedral distortion is also facilitated/promoted by cation−cation repulsion in the face-sharing octahedra.

Although the inherent limitations in X-ray powder diffraction prevent a detailed analysis of the trends in bond distances that could be examined in crystal structures obtained from single-crystal diffraction or neutron powder diffraction data, the changes in (Ru/Ir)−(Ru/Ir) bond distances may, nonetheless, be investigated with powder X-ray diffraction data when the average oxidation state of the cation in the face-sharing octahedra is considered. The (Ru/Ir)−(Ru/Ir) bond distances of 2.777(3) Å for $Ba_3LiIrRuO_9$ are comparable to the *d*(Ir−Ir) of 2.7563(6) Å for $Ba_3LiIr_2O_9$ and the *d*(Ru−Ru) of 2.768(1) Å for $Ba_3LiRu_2O_9$.[13,20] Similarly, the (Ru/Ir)−(Ru/Ir) bond distances of 2.731(3) Å for $Ba_3NaIrRuO_9$ are comparable to 2.7253(2) Å for $Ba_3NaIr_2O_9$ and 2.7482(9) Å for $Ba_3NaRu_2O_9$.[13,20] The (Ru/Ir)−(Ru/Ir) bond distances for the mixed iridium−ruthenium triple perovskites investigated in this study range from 2.57 to 2.78 Å, and similar bond distances were observed for the all-iridate or -ruthenate end compositions. It is noteworthy that larger (Ru/Ir)−(Ru/Ir) bond distances were found for $Ba_3MRuIrO_9$ where M = Li and Na [average oxidation state (Ru/Ir) = +5.5] than where M = Mg, Ni, and Zn [average oxidation state (Ru/Ir) = +5.0], which were longer than where M = Bi, In [average oxidation state (Ru/Ir) = +4.5]. These trends in (Ru/Ir)−(Ru/Ir) bond distances are consistent with increased cation−cation repulsion as the average oxidation state of the dimer cations is increased. Some of the (Ru/Ir)−(Ru/Ir) bond distances were obtained from crystal data of $Ba_3LnRuIrO_9$ in the accompanying paper.[22] The (Ru/Ir)−(Ru/Ir) bond distances

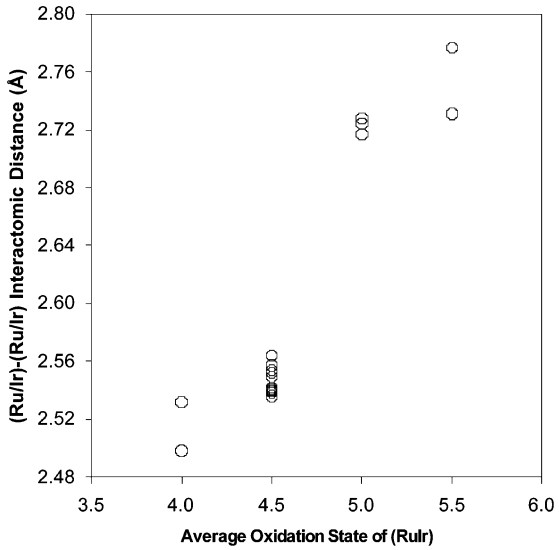

Figure 3. (Ru/Ir)−(Ru/Ir) bond distance versus average oxidation state of the dimer cations.

(22) Lufaso, M. W.; zur Loye, H. C. *Inorg. Chem.* **2005**, *44*, 9143−9153.

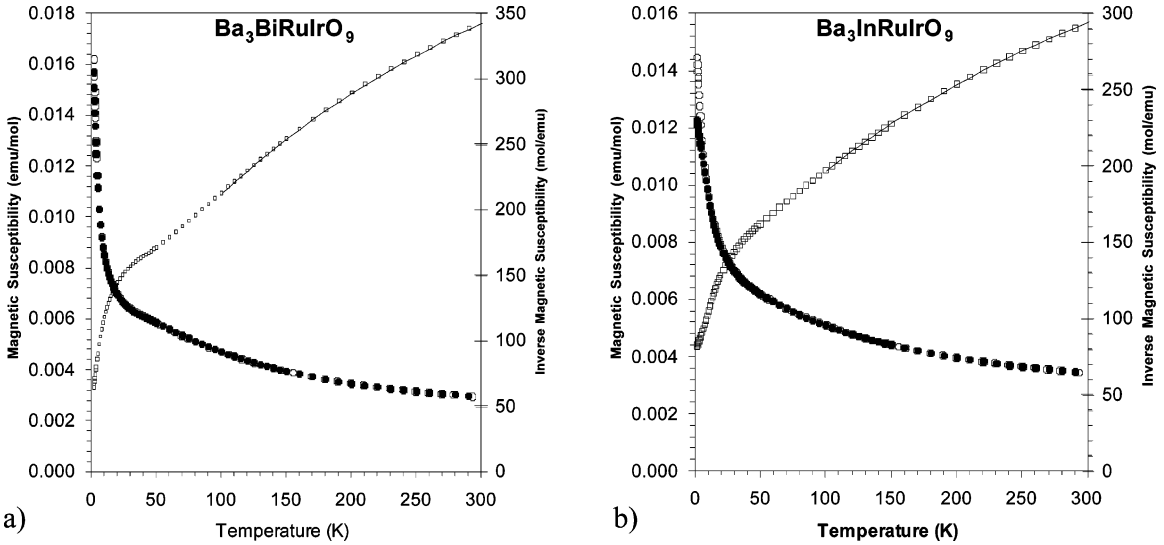

Figure 4. Temperature dependence of the zero-field-cooled (filled circle) and field-cooled (open circle) magnetic susceptibilities and (open square) inverse magnetic susceptibility at an applied field of 1 kG for (a) $Ba_3BiRuIrO_9$ and (b) $Ba_3InRuIrO_9$.

arranged by average oxidation state of the cation in the face-sharing dimer are shown in Figure 3. The shortest (Ru/Ir)−(Ru/Ir) separation occurs for the tetravalent average oxidation state, whereas larger separations of the (Ru/Ir)−(Ru/Ir) cations are found for the higher average oxidation states (4.5+, 5.0+, 5.5+) of the metals in the dimer. These trends in bond distances in the face-sharing dimer are also consistent with the observed increased octahedral distortion and increased cation−cation repulsion in compounds with higher average oxidation states of the dimer cations. The off-center displacement, Δ, is defined as the distance the Ru/Ir is displaced from the position ($^1/_3$, $^2/_3$, $^1/_6$), tends to increase with average oxidation state of the dimer cations, and is given in Table 3.

3.b. Magnetic Susceptibility. To investigate the possible existence of magnetic interactions in the mixed iridium−ruthenium perovskites, the magnetic susceptibilities were examined as a function of temperature. The temperature dependence of the ZFC and FC magnetic susceptibilities for $Ba_3MIrRuO_9$ (M = In, Bi) is shown in Figure 4 and that for $Ba_3MIrRuO_9$ (M = Mg, Ni, Zn, Li) in Figure 5. Using the ZFC data, we calculated the μ_{eff} values at 300 K using eq 1 where k_B is Boltzmann's constant and N_A is Avogadro's

$$\mu_{eff} = \sqrt{3k_B\chi T/N_A} \qquad (1)$$

number, and these values are listed in Table 4. It is well-known that reduced magnetic moments are often observed in ruthenate and iridate triple perovskites, which has been attributed to spin−orbit coupling and antiferromagnetic exchange interactions in the face-sharing octahedra.[20,23] Attempts to fit the susceptibility data with a standard Curie−Weiss law failed, since the data were nonlinear even in the 150−300 K temperature range. A modified Curie−Weiss law, which includes a term for temperature-independent paramagnetism (χ_{tip}), has been used previously in the analysis of the susceptibility data of triple perovskites.[7,24] The results of the fits are shown as the solid curve in the inverse susceptibility. It should be noted that the values obtained from the susceptibility data are approximate values, since the susceptibilities are nonlinear in the temperature range of this study. Curie constants (C), Weiss constants (θ), and χ_{tip} values obtained from the fitting of the magnetic susceptibility data are given in Table 4. The μ_{eff} (fit) was calculated from the fitted Curie constant. The χ_{tip} values obtained in the fitting procedure were on the order of 10^{-3} emu/mol. Although the sizes of the χ_{tip} values are considerable, they are comparable to values previously observed in magnetic studies of triple perovskites.[24]

3.b.i. $Ba_3MRuIrO_9$ (M = In, Bi). ZFC and FC magnetic susceptibilities of $Ba_3InRuIrO_9$ and $Ba_3BiRuIrO_9$ are shown in Figure 4. The shape of the inverse susceptibilities is nonlinear up to 300 K, which is similar to what is observed for $Ba_3YRuIrO_9$, $Ba_3LuRuIrO_9$, and $Ba_3LaRuIrO_9$ and which is reported in the accompanying article.[22] A Curie−Weiss law with a temperature-independent paramagnetic term was used to fit the susceptibility data. The results from the fitting procedure are reported in Table 4. In the accompanying article, an assignment of the iridium and ruthenium oxidation states of $[Ir^{4+}Ru^{5+}O_9]$ in the dimer was made for the formal oxidation states in $Ba_3M^{3+}RuIrO_9$ triple perovskites. An analogous assignment of oxidation states was made and used for the compounds presented in this paper.

The published magnetic measurements of $Ba_3BiRu_2O_9$ exhibited a sharp downturn in the susceptibility near 175 K.[11] In contrast, the magnetic susceptibility of $Ba_3BiRuIrO_9$ does not exhibit any downturn in the temperature range 2−300 K. The effective magnetic moments of $Ba_3InRuIrO_9$ are 2.85 μB at 300 K and 0.44 μB at 2 K. The effective magnetic moments of $Ba_3BiRuIrO_9$ are 2.64 μB at 300 K and 0.50 μB at 2 K. These reduced effective magnetic moments are indicative of antiferromagnetic interactions at low temperatures.

(23) Byrne, R. C.; Moeller, C. W. *J. Solid State Chem.* **1970**, *2*, 228.

(24) Rijssenbeek, J. T.; Matl, P.; Batlogg, B.; Ong, N. P.; Cava, R. J. *Phys. Rev. B* **1998**, *58*, 10315.

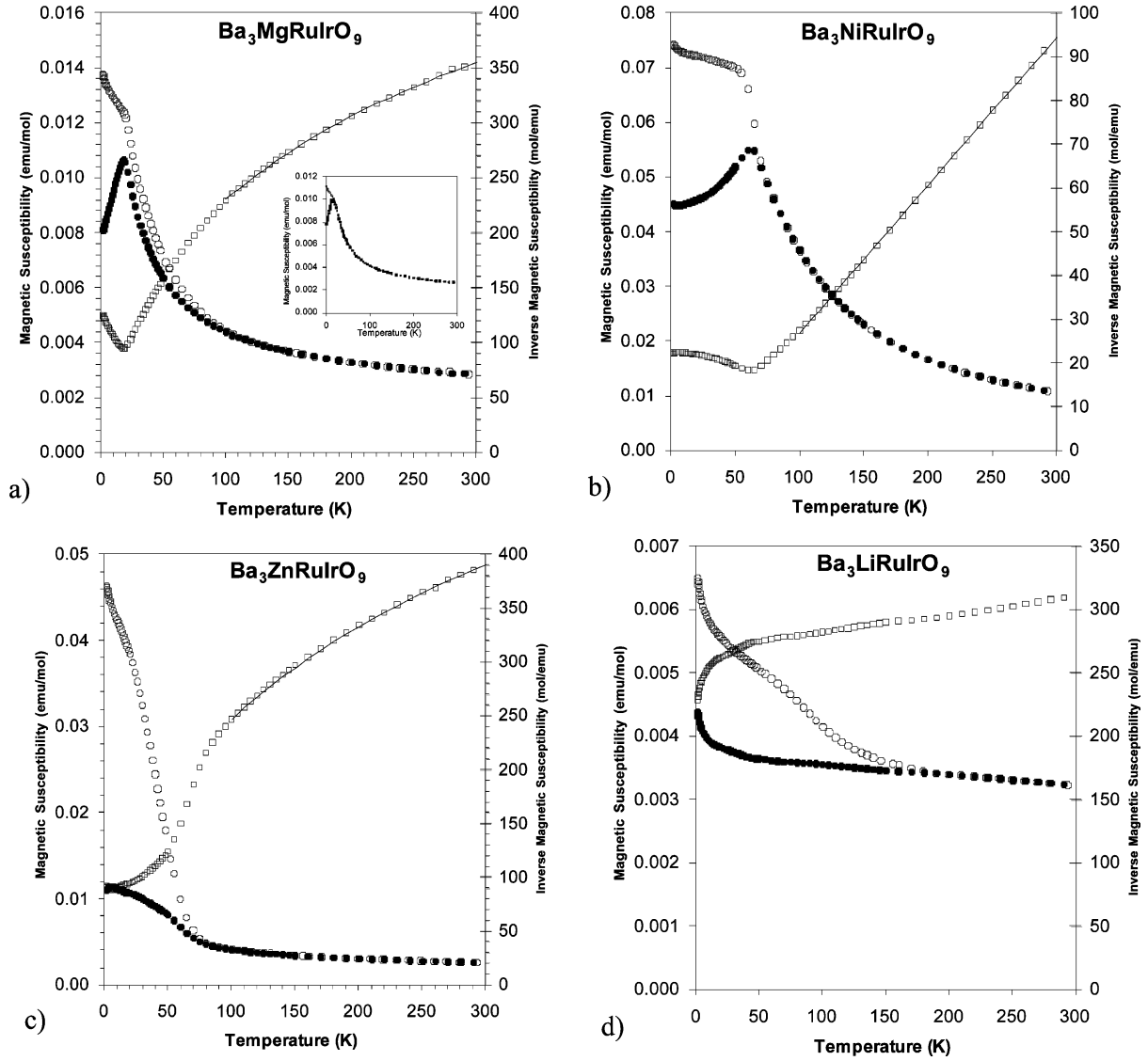

Figure 5. Temperature dependence of the zero-field-cooled (filled circle) and field-cooled (open circle) magnetic susceptibilities and (open square) inverse magnetic susceptibility at an applied field of 1 kG for (a) $Ba_3MgRuIrO_9$, (b) $Ba_3NiRuIrO_9$, (c) $Ba_3ZnRuIrO_9$, and (d) $Ba_3LiRuIrO_9$.

Table 4. Calculated Magnetic Moments Using Each Magnetic Ion (μ_{cal}), Effective Magnetic Moments (μ_{eff}) at 300 K, and the Effective Magnetic Moment from the Fitting of Modified Curie−Weiss Fitting Results in the Temperature Range 100−300 K

	μ_{cal} (μ_B)	μ_{eff} (μ_B) (300 K)	μ_{eff} (μ_B) (fit)	C (emu/mol K)	χ_{tip} (emu/mol)	θ (K)
In	2.29	2.85	2.16(1)	0.586(7)	0.001 87(1)	−82(1)
Bi	2.29	2.65	1.98(2)	0.494(7)	0.001 53(1)	−55(2)
Mg	1.50	2.59	1.75(3)	0.384(14)	0.001 70(3)	−46(4)
Ni	3.20	5.02	4.83(1)	2.956(6)		21.2(4)
Zn	1.50	2.46	1.73(5)	0.378(23)	0.001 47(5)	−47(7)

3.b.ii. $Ba_3MRuIrO_9$ (M = Mg, Ni, Zn). $Ba_3MgRuIrO_9$ exhibits a broad separation of the ZFC and FC susceptibilities starting at about 100 K, as shown in Figure 5a. The inset to Figure 5a shows the ZFC and FC magnetic susceptibilities at an applied field of 10 kG where the broad separation of the ZFC and FC susceptibilities is only present below 19 K. At that temperature, a sharp divergence occurs that is indicative of antiferromagnetic interactions and that agrees well with the negative Curie−Weiss constant of −46(4) K. Similar magnetic behavior of the ZFC and FC magnetic susceptibilities is observed for $Ba_3NiRuIrO_9$ (Figure 5b), where ZFC and FC values diverge near 65 K and exhibit a shape typically associated with the presence of antiferromagnetic correlations. However, the positive Curie−Weiss temperature of 21.2(4) K indicates that there may be ferromagnetic interactions related to the presence of the d^8 Ni^{2+}, which may couple with the dimer cations along the Ni−O2−(Ru/Ir) pathway with a pseudolinear 174.8(5)° bond angle. This observation is in agreement with the prediction that the ∼90° (Ru/Ir)−O−(Ru/Ir) superexchange pathway is antiferromagnetic and the ∼180° Ni^{2+}−O−(Ru/Ir) pathway is ferromagnetic.[25] In comparison, the crystal and magnetic structure of $Ba_3NiRu_2O_9$ determined by neutron powder diffraction indicated a magnetic transition near 100 K, which was determined to be due to long-range antiferromagnetic order.[14,15]

$Ba_3ZnRuIrO_9$ (Figure 5c) shows a divergence of the ZFC and FC susceptibility data near 75 K; however, the difference

(25) Goodenough, J. B. *Magnetism and the Chemical Bond*; Interscience: New York, 1963.

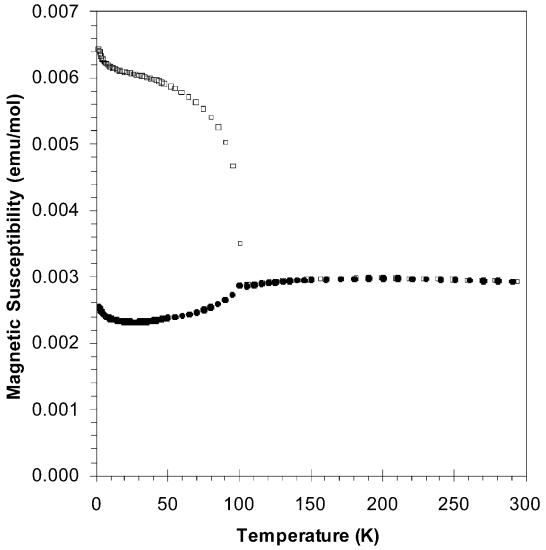

Figure 6. Temperature dependence of the zero-field-cooled (filled circle) and field-cooled (open square) magnetic susceptibilities of $Ba_3NaRuIrO_9$ at an applied field of 500 G.

between the FC and ZFC curves are more subtle than for $Ba_3MgRuIrO_9$ and $Ba_3NiRuIrO_9$ in the applied field used in this study. In a related compound, $Ba_3ZnRu_2O_9$, the ordered Ru^{5+} moment was much smaller compared to those found in $Ba_3NiRu_2O_9$ and $Ba_3CoRu_2O_9$.[15] The susceptibility data indicate antiferromagnetic interactions occur at low temperatures for the $Ba_3MRuIrO_9$ (M = Mg, Ni, Zn) compounds. It is noteworthy that $Ba_3MRu_2O_9$ (M = Mg, Ni, Zn) each showed magnetic hyperfine splitting which could only be interpreted in terms of long-range magnetic order and the absence of an $S = 0$ ground state.[26] Although the magnetism of $Ba_3ZnRuIrO_9$ and $Ba_3MgRuIrO_9$ indicates an effective magnetic moment near that expected for a spin $^1/_2$ system when fitted as a Curie−Weiss-type system, the effective magnetic moments calculated as a function of temperature vary significantly and prevent treating the magnetism as a molecular orbital picture for a dimeric cluster $[IrRuO_9]^{8-}$ that has been used to examine the face-shared trioctahedra in the structurally related $Ba_3MnRu_2O_9$.[10]

3.b.iii. $Ba_3MRuIrO_9$ (M = Li, Na). The average oxidation state of (Ru/Ir) in $Ba_3MRuIrO_9$ is 5.5+. In part 1 of this work, the formal oxidation states in $Ba_3M^{3+}RuIrO_9$ were assigned as Ir^{4+} and Ru^{5+}.[22] By analogy, the formal oxidation states are presumed to be $Ba_3M^{1+}Ru^{6+}Ir^{5+}O_9$ (M = Li, Na). Examples of oxide compounds containing Ru^{6+} are relatively uncommon but include Na_2RuO_4,[27] $Ba_5Na_2Ru_3O_{14}$,[28] $Sr_2Ru_3O_{10}$,[29] $BaHgRuO_5$,[30] $CsK_5Ru_2O_9$,[31] Cs_2RuO_4,[32] $Ba_3LiRu_2O_9$,[20] and $Ba_3NaRu_2O_9$.[20] Interesting behavior, including a charge ordering and crystallographic phase transition accompanied by a drop in the susceptibility near 210 K,[13] was observed for $Ba_3NaRu_2O_9$. In the isostructural $Ba_3NaIr_2O_9$, a divergence of the ZFC and FC data occurs in the magnetic susceptibility data near 50 K.[20] The temperature dependence of the zero-field-cooled and field-cooled magnetic susceptibilities and inverse magnetic susceptibility at an applied field of 500 G of $Ba_3NaRuIrO_9$ is given in Figure 6. A sharp transition is indicated for $Ba_3NaRuIrO_9$ near 100 K, and above this temperature, the susceptibility is approximately independent of temperature, which suggests the possibility for a nonlocalized spin system.

$Ba_3LiRuIrO_9$ exhibited a divergence of the ZFC and FC data near 180 K, as shown in Figure 5d. By comparison, a divergence of the ZFC and FC data occurs in the magnetic susceptibility data near 75 K for $Ba_3LiIr_2O_9$.[20] A decrease in the susceptibility near 140 K was observed for $Ba_3LiRu_2O_9$.[13] The magnetic susceptibility curve of $Ba_3LiRuIrO_9$ did not have a temperature dependence similar to that of either of the two end-member compounds. Furthermore, the divergence in the susceptibility data of $Ba_3LiRuIrO_9$ occurs at a higher temperature than any divergence in the susceptibility of either end member. A large negative Weiss constant, ∼−1830 K, indicates strong antiferromagnetic interactions. The effective magnetic moments at 2 and 300 K are 0.26 and 2.77 μ_B. An estimation of the spin-only moment is calculated using noninteracting Ir^{5+} and Ru^{6+}, each with spin-only moments of 2.83 μ_B. The spin-only predicted effective magnetic moment, 4.0 μ_B, is larger than the measured effective moments. The reduced moment is attributed to a combination of spin−orbit coupling and antiferromagnetic exchange interactions in the disordered face-sharing octahedra.

4. Conclusions

The quinternary oxides $Ba_3MRuIrO_9$ (M^{1+} = Li, Na; M^{2+} = Mg, Ni, Zn; M^{3+} = Bi, Y, In, lanthanides; M^{4+} = Tb, Pr) have a 6H-$BaTiO_3$-related crystal structure in which $Ba_3BiRuIrO_9$ crystallizes in space group *C*2/*c* and the others in space group $P6_3/mmc$. Short bond distances are present between the disordered (Ir/Ru) in the face-sharing dimer ranging from 2.58 to 2.78 Å. The (Ru/Ir)−(Ru/Ir) interatomic distances increase for a higher average oxidation state of the dimer cations, which is attributed to increased cation−cation repulsion and optimization of the coordination environment for the oxygen atoms in the asymmetric bond network. $Ba_3BiRuIrO_9$ and $Ba_3InRuIrO_9$ exhibit magnetic behavior similar to that of previously examined $Ba_3M^{3+}RuIrO_9$ triple perovskites, and the formal oxidation states may be assigned at Ru^{5+} and Ir^{4+}. $Ba_3MRuIrO_9$ (M = Mg, Ni, Zn) show a divergence of the ZFC and FC data over a wide temperature range. The ZFC and FC data of $Ba_3LiRuIrO_9$ exhibit a broad deviation over a wide temperature range, starting near 160 K. $Ba_3MRuIrO_9$ compounds, as a function *M*, can exhibit a wide range of average oxidation states (4+ to 5.5+) for the disordered cations in the face-sharing octahedra and exhibit diverse magnetic properties. The disorder present in the face-

(26) Fernandez, I.; Greatrex, R.; Greenwood, N. N. *J. Solid State Chem.* **1980**, *34*, 121.
(27) Shikano, M.; Kremer, R. K.; Ahrens, M.; Koo, H. J.; Whangbo, M. H.; Darriet, J. *Inorg. Chem.* **2004**, *43*, 5.
(28) Quarez, E.; Mentre, O. *Solid State Sci.* **2003**, *5*, 1105.
(29) Renard, C.; Daviero-Minaud, S.; Abraham, F. *J. Solid State Chem.* **1999**, *143*, 266.
(30) Hansen, T.; LeBail, A.; Laligant, Y. *J. Solid State Chem.* **1995**, *120*, 223.
(31) Fischer, D.; Hoppe, R. *Z. Anorg. Allg. Chem.* **1994**, *617*, 37.
(32) Fischer, D.; Hoppe, R. *Z. Anorg. Allg. Chem.* **1990**, *591*, 87.

sharing octahedra leads to a mixture of possible magnetic interactions, which makes a quantitative description of the magnetic properties difficult. In a manner similar to what is observed for the end-member ruthenate and iridate perovskites, there are antiferromagnetic interactions within the face-sharing octahedral dimer.

Acknowledgment. Financial support from the Department of Energy through Grant DE-FG02-04ER46122 and the National Science Foundation through Grant DMR: 0450103 is gratefully acknowledged.

IC051345R